Ionics (2023) 29:3385–3392
https://doi.org/10.1007/s11581-023-04993-1

RESEARCH

Development of rutin sensor based on graphene quantum dots@nano-carbon ionic liquid electrode

Xinsheng Liu[1] · Wenli Qiao[2] · Mengjun Chang[2] · Yan Wang[2] · Yonghong Li[2,3]

Received: 23 February 2023 / Revised: 27 March 2023 / Accepted: 9 April 2023 / Published online: 24 April 2023

Abstract

A graphene quantum dots@nano-carbon ionic liquid electrode was prepared (GQDs@nano-CILE) to detect rutin sensitively. The graphene quantum dots were characterized by transmission electron microscopy (TEM) and infrared spectroscopy (IR). The surface morphology of the modified electrode was studied by scanning electron microscope (SEM). Cyclic voltammetry (CV) was used to investigate the electrochemical properties and the effective surface area of the modified electrodes. The effects of solution pH value, accumulation potential, and time on peak current were also discussed. Compared with nano-carbon paste electrode (nano-CPE), the peak current of rutin on GQDs@nano-CILE increased significantly using differential pulse voltammetry (DPV). The linear range of rutin ranging from 5×10^{-9} to 1×10^{-5} mol L^{-1} was obtained under the optimized conditions. The detection limit was 2×10^{-9} mol L^{-1} (S/N = 3). The modified electrode could be used for rutin analysis in rutin tablets and urine samples, and the recovery was between 95.2 and 101.4%.

Keywords Ionic liquid · Graphene quantum dots · Nano-carbon paste electrode · Rutin

Introduction

Rutin belongs to vitamin P, which is a bioactive flavonoid compound. Rutin can be extracted from such plants as rue leaf, tobacco leaf, jujube, apricot, orange peel, tomato, buckwheat flower, and so on. Rutin has significant medicinal value and plays a vital role in clinical treatment, such as anti-oxidation, anti-diabetes, anti-fat, neuroprotective, and hormone therapeutic effects [1, 2]. Furthermore, rutin is also the primary raw material for synthesizing troxerutin. Troxerutin is used as a cardiovascular and cerebrovascular drug, which can effectively inhibit the aggregation of platelets and prevent thrombosis. Therefore, it is significant for analyzing rutin content in drug quality control fields.

Currently, the methods for the determination of rutin include high-performance liquid chromatography (HPLC) [3], capillary electrophoresis (CE) [4, 5], ultraviolet spectrophotometry (UV) [6, 7], electrochemiluminescence (EL) [8], and electrochemical method (EC) [9–11]. By contrast, electrochemical methods have some advantages such as fast response, high sensitivity, simple instrument, and easy operation. To improve the electrochemical performance of the modified electrode, various materials with excellent properties are utilized to modify the bare electrode. Graphene quantum dots (GQDs) are a new type of graphene-based carbon nanomaterial. Compared with traditional semiconductor quantum dots, GQDs have the advantages of good biocompatibility, easy binding with biomolecules, and low biotoxicity [12]. At the same time, GQDs exhibit a large surface area and high electron mobility [13, 14]. They also have the properties of photoluminescence (PL) by quantum confinement and edge effect [15], which have great application potential in the construction of electrochemical sensors and fluorescence sensors. Ionic liquids are room-temperature molten salts, mainly composed of organic cations and anions. The ionic liquids possess good electric catalytic activity, high ionic conductivity, stable chemical properties, and wide electrochemical window [16, 17]. Due to these excellent

✉ Yonghong Li
yonghongli2012@163.com

[1] School of Basic Medical Sciences, Ningxia Medical University, Yinchuan 750004, People's Republic of China

[2] School of Public Health, Ningxia Medical University, Yinchuan 750004, People's Republic of China

[3] Key Laboratory of Environmental Factors and Chronic Disease Control, Yinchuan 750004, People's Republic of China

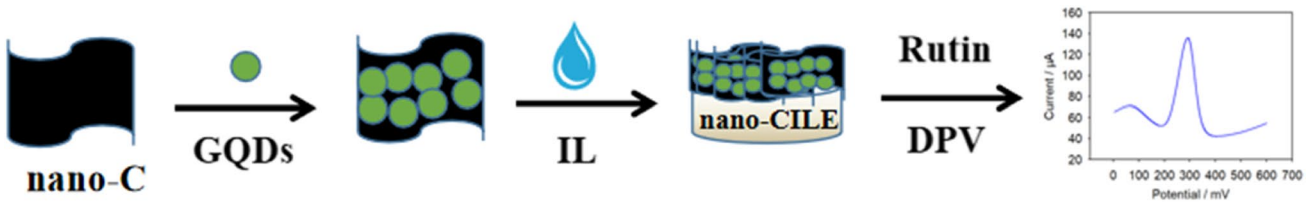

Scheme 1 The fabrication procedure of GQDs@nano-CILE and the electrochemical process of rutin

performances, ionic liquids are widely used for preparing electrochemical sensors, exhibiting low cost, easy surface modification, high sensitivity and selectivity, and good anti-fouling ability. The graphene quantum dots-ionic liquid composites can improve the electrochemical performance of the sensor, increasing the current response signal.

In this paper, a graphene quantum dots@nano-carbon ionic liquid electrode (GQDs@nano-CILE) was constructed in a simple preparation process for sensing rutin. The effective surface area of the sensor was discussed by scan rate study. The electrochemical behavior of rutin on GQDs@nano-CILE was studied by differential pulse voltammetry (DPV), and its reaction mechanism was also discussed. The established method was successfully utilized to detect rutin in urine samples and rutin tablets.

Experimental

Reagents and materials

Graphite powder, paraffin oil, and rutin were obtained from Sinopharm Chemical Reagent Co., Ltd. Nano-graphite powder (sheet diameter: ~ 400 nm, thickness: < 40 nm), and graphene quantum dots (GQDs, 1 mg mL^{-1}) was purchased from Nanjing XFNANO Materials Tech Co., Ltd. Ionic liquid (1-octylpyridine hexafluorophosphate, $OPPF_6$) was supplied by Lanzhou Yulu Fine Chemical Co. Ltd. Rutin tablets were produced by Yunpeng Pharmaceutical Co., Ltd.

Rutin standard solution was prepared by dissolving a standard substance in ethanol solution. 0.1 M phosphate buffer (PBS) was used as the supporting electrolyte. All other reagents were of analytical grade and were not further purified before use. Ultrapure water (18.2 MΩ·cm) was used throughout the experiment.

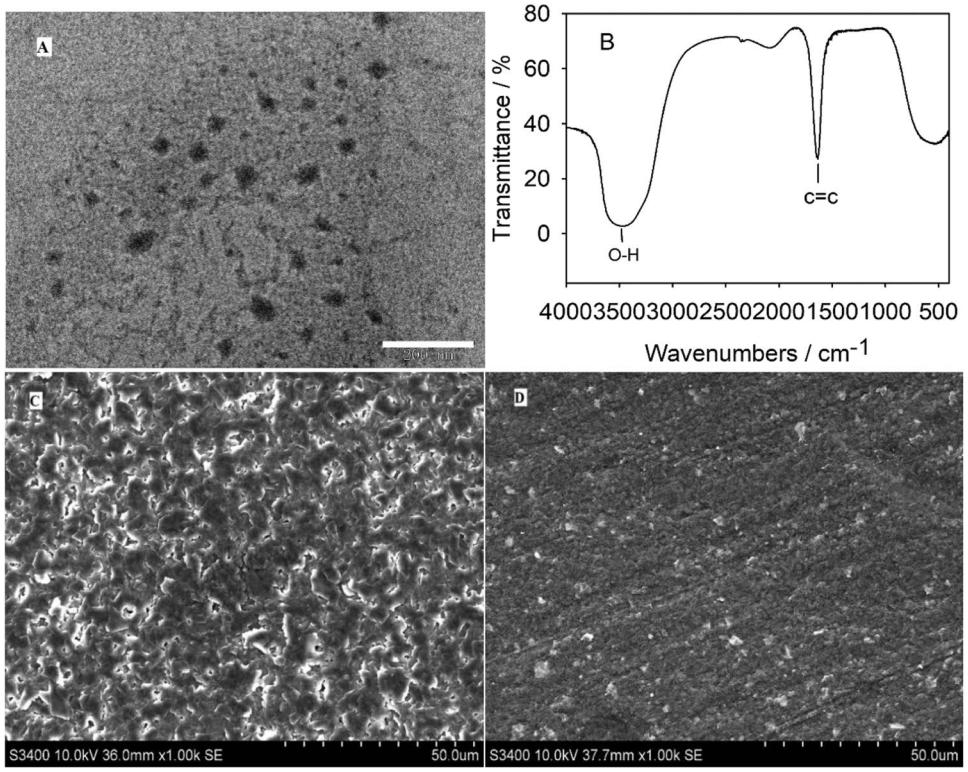

Fig. 1 **A** TEM image of GQDs; **B** FTIR absorbance spectra of GQDs; SEM images of nano-CPE (**C**) and GQDs@nano-CILE (**D**)

Apparatus

Cyclic voltammetry (CV) and differential pulse voltammetry (DPV) were performed on a CHI 660E electrochemical workstation (Shanghai Chenhua Instrument Co., Ltd. China). The three-electrode system consists of a modified electrode, a Pt wire electrode, and a saturated calomel electrode. The magnetic agitator (IKA KMO2) was used in the preconcentration process. The morphology of graphene quantum dots (GQDs) was obtained by transmission electron microscopy (HITACHI H-7650, Tokyo, Japan). The scanning electron micrographs (SEM) of the modified electrodes were obtained with a Hitachi S-3400 scanning electron microscope (Hitachi Ltd., Tokyo, Japan). IR spectra were recorded on an IRAffinity-1 Fourier transform infrared (FTIR) spectrophotometer (Shimadzu Co., Ltd., Japan).

Electrode preparation

Firstly, graphene quantum dots@nano-graphite powder composites (GQDs@nano-C) were synthesized according to the following steps: 750 µL graphene quantum dots solution was evenly mixed with 1 g nano-graphite powder and dried under room temperature for later use.

The graphene quantum dots@nano-carbon ionic liquid electrode (GQDs@nano-CILE) was prepared according to the following method: First, 0.05 g GQDs@nano-C composites and 0.05 g ionic liquid ($OPPF_6$) were mixed uniformly in an agate mortar, then a certain amount of carbon paste was squeezed into a Teflon tube (3 mm diameter). After being heated with a hair drier, the prepared electrode was polished on the weighing paper to obtain a new electrode surface.

The traditional carbon paste electrode (CPE) was prepared by mixing graphite powder with paraffin oil. By contrast, the nano-carbon paste electrode (nano-CPE) was composed of nano-graphite powder and paraffin oil. Nano-carbon ionic liquid electrode (nano-CILE) consisted of nano-graphite powder and ionic liquid.

Analytical procedure

The electrochemical performance of the sensor was studied by cyclic voltammetry (CV) in 5 mM $K_3[Fe(CN)_6]$/$K_4[Fe(CN)_6]$ and 0.1 M KCl solution. The CVs were recorded from − 0.2 to 0.6 V with a scan rate of 50 mV s^{-1}. The differential pulse voltammetry (DPV) was utilized to discuss the electrochemical behavior of rutin in 0.1 M PBS (pH 6.0). The DPVs were recorded in the range of 0–0.6 V with an accumulation time of 10 s at open circuit potential. The modified electrode was washed with ultrapure water after every measurement. Scheme 1 exhibits the fabrication procedure of GQDs@nano-CILE and the electrochemical sensing process of rutin.

Results and discussion

Surface morphology and structure characterization

The structure of GQDs was characterized using transmission electron microscopy (TEM). As shown in Fig. 1A, the GQDs exhibited spherical shapes, and their plane sizes were less than 50 nm. Fourier transform infrared spectroscopy was also used to investigate GQDs. Figure 1B exhibits the FTIR spectra of GQDs. The O–H stretching vibration absorption peak on GODs was at about 3444.87 cm^{-1}. The vibration absorption peaks of C = C appeared at 1635.64 cm^{-1}. The results showed that hydrophilic hydroxyl groups were attached on the surface of GQDs, which was beneficial to the formation of intermolecular hydrogen bonds with rutin. The nano-CPE (shown in Fig. 1C) presented an unsmooth surface with some gaps. As exhibited in Fig. 1D, when ionic liquids were used as the binder, a uniform surface morphology could be observed on the GQDs@nano-CILE. The ionic liquid could act as bridges to connect the discontinuity between carbon materials.

Electrochemical characterization

Figure 2 shows CVs of different electrodes in 5 mM $[Fe(CN)_6]^{3-/4-}$ and 0.1 M KCl solution. As shown in the figure, the relationship on the redox peak potential difference (ΔEp) of different electrodes was as follows: GQDs@nano-CILE < nano-CILE < GQDs @ nano-CPE < nano-CPE < CPE. Since the electron transfer rate increased with the decrease of ΔEp, GQDs@nano-CILE presented the fastest electron transfer rate. At the same time, the order of the oxidation peak current (I_{pa}) on different

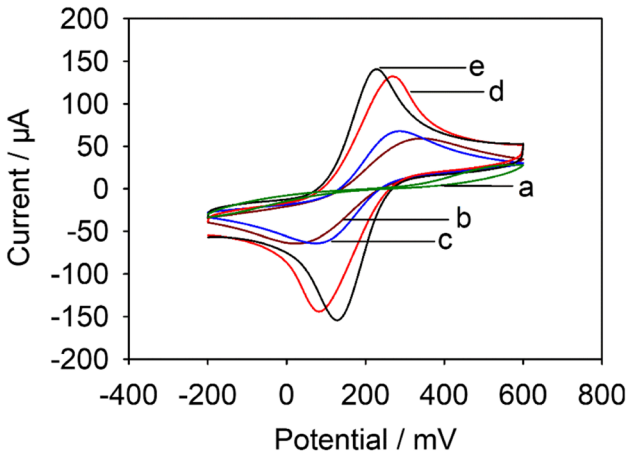

Fig. 2 CVs of (**a**) CPE; (**b**) nano-CPE; (**c**) GQDs@nano-CPE; (**d**) nano-CILE; (**e**) GQDs@nano-CILE in 5 mM $[Fe(CN)_6]^{3-/4-}$ solution containing 0.1 M KCl

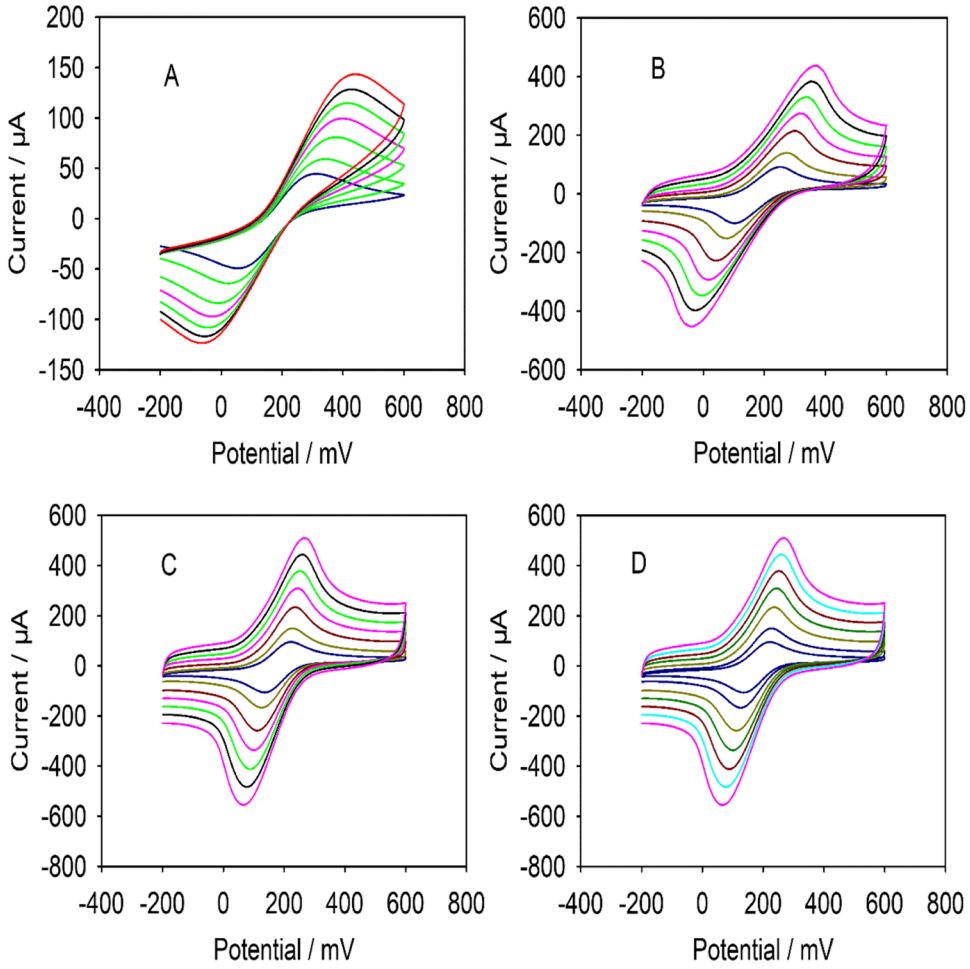

Fig. 3 CVs of 5 mM $[Fe(CN)_6]^{3-/4-}$ and 0.1 M KCl solution at various scan rates on **A** nano-CPE; **B** GQDs@nano-CPE; **C** nano-CILE; **D** GQDs@nano-CILE. The scan rates are 25, 50, 100, 150, 200, 250, and 300 mV $s.^{-1}$, respectively (from inner to outer)

electrodes was as follows: GQDs@nano-CILE > nano-CILE > GQDs@nano-CPE > nano-CPE > CPE. The phenomenon was due to the synergistic effect of graphene quantum dots and ionic liquids. The modified electrode exhibited improved electrochemical performance with good adsorbability and high conductivity.

Surface area study

Figure 3 displays CVs of the modified electrodes at different scan rates in 5 mM $[Fe(CN)_6]^{3-/4-}$ solution. The anode peak current (I_{pa}) was linearly increased with the square root of scan rate ($v^{1/2}$), and the linear equations were I (μA) = 192.3132 $v^{1/2}$ ($V^{1/2}$ $s^{-1/2}$) + 10.7774 (r^2 = 0. 9967) for nano-CPE; I (μA) = 231.7864 $v^{1/2}$ ($V^{1/2}$ $s^{-1/2}$) + 12.5002 (r^2 = 0. 9974) for GQDs@nano-CPE; I (μA) = 381.5616 $v^{1/2}$ ($V^{1/2}$ $s^{-1/2}$) + 33.2187 (r^2 = 0. 9987) for nano-CILE; I (μA) = 613.0998 $v^{1/2}$ ($V^{1/2}$ $s^{-1/2}$) + 8.3232 (r^2 = 0. 9960) for GQDs@nano-CILE, respectively. For a reversible reaction, the relationships between anodic peak current (I_p) and scan rate (ν) can be described as follows [18]:

$$I_p = \left(2.69 \times 10^5\right) n^{3/2} A C_0 {D_R}^{1/2} v^{1/2} \quad (1)$$

where n is the electron transfer number (n = 1), A is the effective surface area of the electrode, C_0 refers to the concentration of

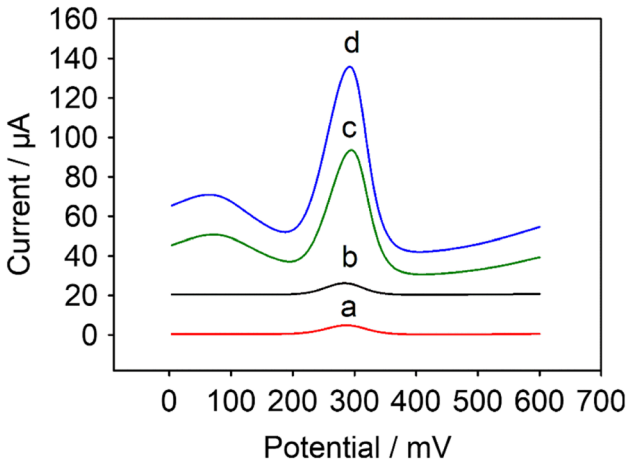

Fig. 4 DPVs of 10 μM rutin on different electrodes: (**a**) nano-CPE; (**b**) GQDs@nano-CPE; (**c**) nano-CILE; (**d**) GQDs@nano-CILE

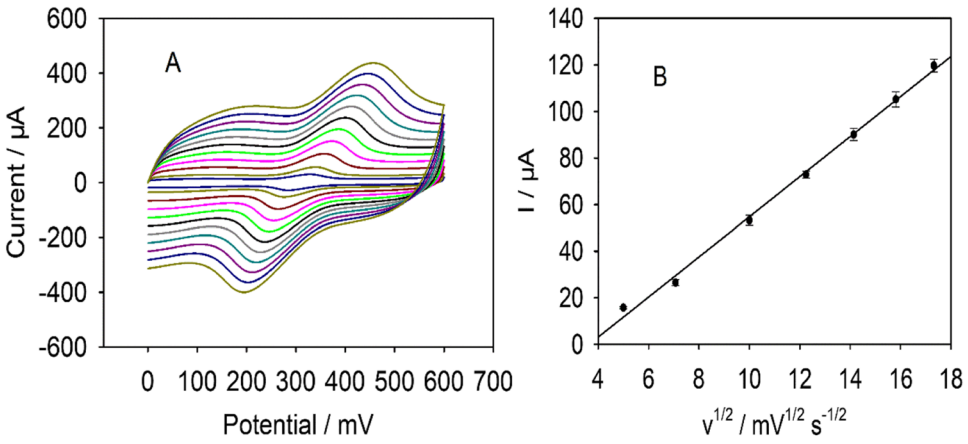

Fig. 5 **A** CVs of 10 μM rutin with various scan rates on GQDs@nano-CILE. The scan rates from inside to outside are 25, 50, 100, 150, 200, 250, and 300 mV s^{-1}. **B** The relationship between peak current and the square root of scan rate

$K_3Fe(CN)_6$ (5×10^{-3} mol L^{-1}), and D_R is diffusion coefficient (6.50×10^{-6} cm^2 s^{-1}). According to the slope of Ip vs. $\nu^{1/2}$ relation, the effective surface areas of nano-CPE, GQDs@nano-CPE, nano-CILE, and GQDs@nano-CILE were calculated to be 0.052 cm^2, 0.062 cm^2, 0.103 cm^2, and 0.165 cm^2, respectively. The GQDs@nano-CILE exhibited the improved effective surface area, suggesting the good adsorbability of the sensor.

Electrochemical behavior of rutin

Figure 4 demonstrates DPVs of 10 μM rutin on nano-CPE, GQDs@nano-CPE, nano-CILE, and GQDs@nano-CILE. A small oxidation peak (about 4.54 μA) could be observed on the nano-CPE (curve a). However, the peak current of rutin was obviously increased (about 5.823 μA) on GQDs@nano-CPE (curve b). Furthermore, the peak current of rutin on nano-CILE (curve c) significantly increased to 59.39 μA, indicating that the high conductive ionic liquid used as the binder could effectively promote the electron transfer rate of rutin. In combination with the excellent properties of graphene quantum dots and ionic liquids, the current response of rutin on GQDs@nano-CILE (curve d) further increased; its peak current (about 88.65 μA) was 19.5 times more than that on the nano-CPE. In addition, the oxidation peak of rutin occurred at about 0.292 V on GQDs@nano-CILE. Compared with nano-CILE, the oxidation peak potential of rutin moved negatively. The results showed that GQDs@nano-CILE had good electrocatalytic activity to rutin.

Effect of scan rate

Figure 5A displays CVs of 10 μM rutin at different scan rates on GQDs@nano-CILE. The oxidation peak current increased with the increase of scan rate. As can be seen from Fig. 5B, the peak current was linearly increased with the square root of scan rate. The linear equation was I (μA) = 8.6117 $\nu^{1/2}$ ($mV^{1/2}$ $s^{-1/2}$) − 31.3310 (r^2 = 0.9964), indicating that the electrochemical reaction of rutin on GQDs@nano-CILE was controlled by diffusion.

Optimization of experimental parameters

Effect of pH value

The effects of pH value on the peak potential and peak current of rutin were investigated. Figure 6A shows DPVs of 10 μM rutin in 0.1 M PBS with different pH values. In the

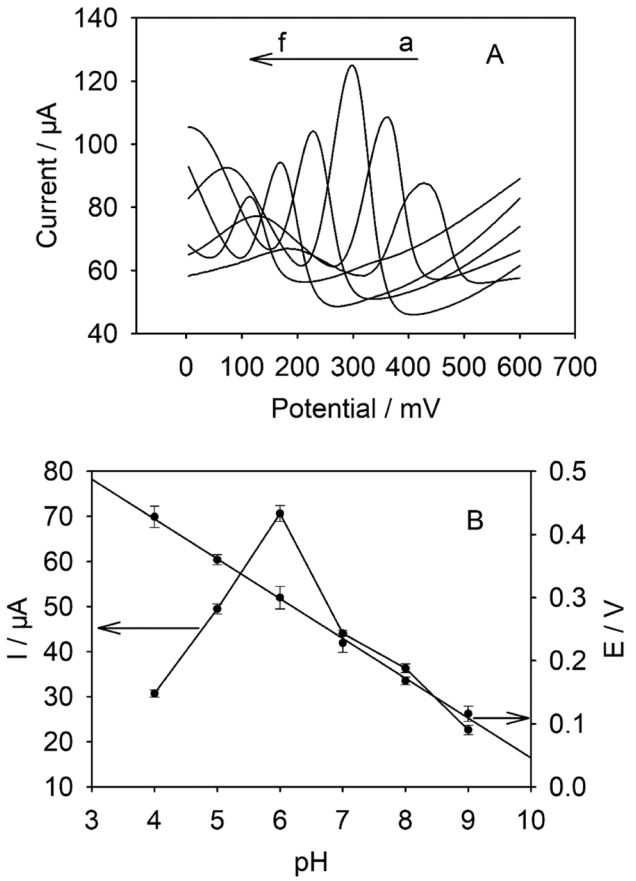

Fig. 6 **A** DPVs of 10 μM rutin with various pH values in 0. 1 M PBS (pH a–f: 4, 5, 6, 7, 8, 9); **B** The effects of pH values on peak current and peak potential of 10 μM rutin on GQDs@nano-CILE

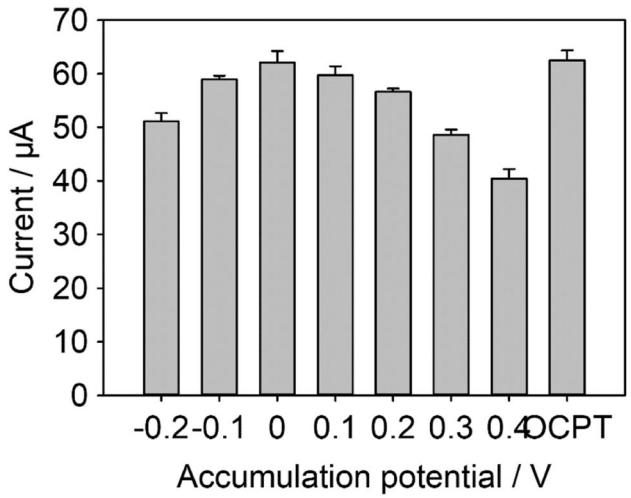

Fig. 7 The effects of accumulation potential and open circuit potential on peak current of 10 μM rutin

range of pH 4–9, the peak current of rutin first increased and then decreased. The maximum current was obtained at pH 6. In addition, the peak potential of rutin gradually moved negatively with the increase of pH. There was a good linear relationship between pH and peak potential (E); the linear equation was E (V) = − 0.0631pH + 0.6767. The slope of 63.1 mV pH^{-1} indicated an equal proton-electron transfer process was involved in the electrode reaction [19].

Effect of accumulation potential

The effects of accumulation potential and open circuit potential (OCPT) on the peak current of rutin were also studied. It could be seen from Fig. 7 that the peak current of rutin first increased and then decreased with the increase of the accumulation potential in the range of − 0.2 to 0.4 V. The maximum peak current was obtained at 0 V. However, the comparable peak current could be observed under OCPT. Therefore, OCPT was selected in the follow-up experiment.

Determination of rutin

A series of rutin standard solutions were determined by DPV under OCPT. As shown in Fig. 8, the oxidation peak current of rutin was linear with the concentration from 5×10^{-9} to 1×10^{-5} mol L^{-1}. The linear equation was I (μA) = 7.1437C (μM) + 1.1844 ($r^2 = 0.9993$), and the detection limit was 2×10^{-9} mol L^{-1} (S/N = 3). Table 1 compares the analytical parameters of different modified electrodes for rutin determination. Compared with other methods [20–23], the constructed sensor in this work exhibited high sensitivity and wide linear range.

Reproducibility and selectivity

The reproducibility of GQDs@nano-CILE was estimated. The relative standard deviation (RSD) of 10 μM rutin for 6 measurements was 3.23% using the same modified electrode. At the same time, the RSD of 6 electrodes prepared in the same procedure for measuring 10 μM rutin was 4.14%. The results indicated that the constructed sensor had good reproducibility.

The influence of potential interfering substances on the determination of rutin was investigated. The results showed that 500 times of K^+, Na^+, Ca^{2+}, Zn^{2+}, Mg^{2+}, 200 times glucose, sucrose, tyrosine, uric acid, 100 times ascorbic acid, Fe^{2+}, 10 times dopamine, the same amount of quercetin and luteolin did not interfere with the current response of 10 μM rutin (peak current change < ± 5%). This phenomenon may be attributed to the following reason: The GQDs have hydrophilic hydroxyl groups on their surface, which was beneficial to the formation of intermolecular hydrogen bonds with rutin.

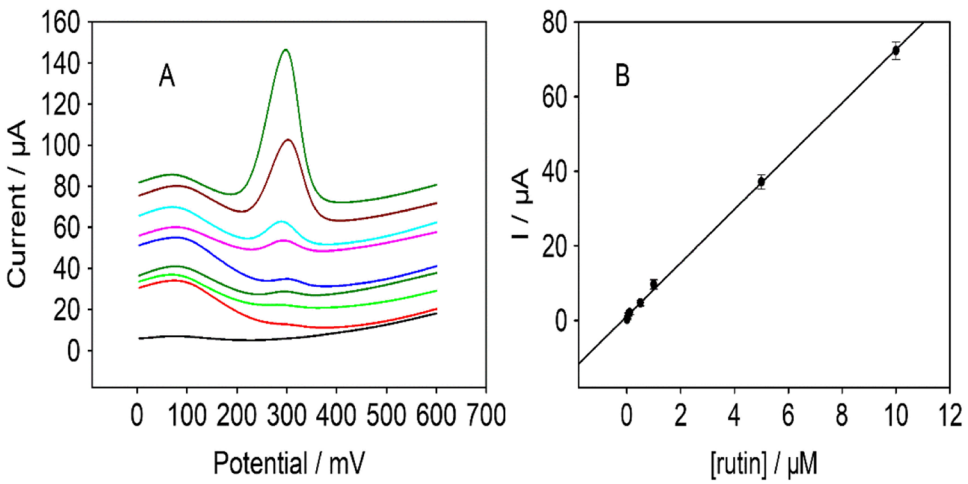

Fig. 8 **A** DPVs of various concentrations of rutin (from bottom to top are 0, 0. 005, 0. 01, 0. 05, 0. 1, 0. 5, 1, 5, 10 μM); **B** The relationship between peak current and concentration of rutin

Table 1 Comparison of analytical performance of different modified electrodes for rutin determination

Electrode	Methods	Linear range / M	Detection limit/ M	Reference
MIP/G[a]-MWCNTs[b]/GCE[c]	DPV[i]	1.0×10^{-8}–1.0×10^{-6}	5.0×10^{-9}	[20]
PdPc[d]-MWCNTs-Nafion/GCE	DPV	1.0×10^{-7}–5.1×10^{-5}	7.5×10^{-8}	[21]
GO-Cs[e]/GCE	DPV	9.0×10^{-7}–9.0×10^{-5}	5.6×10^{-7}	[22]
PdAu/RGO[f]/GCE	DPV	2.5×10^{-8}–5.625×10^{-6}	2.5×10^{-8}	[23]
GQDs[g]@nano-CILE[h]	DPV	5.0×10^{-9}–1.0×10^{-5}	2.0×10^{-9}	This work

[a]Molecular imprinting graphene
[b]Multiwall carbon nanotubes
[c]Glassy carbon electrode
[d]Palladium phthalocyanine
[e]Graphene oxide-chitosan
[f]PdAu/reduced graphene oxide
[g]Graphene quantum dots
[h]Nano-carbon ionic liquid electrode
[i]Differential pulse voltammetry

Actual sample analysis

To verify the practical application ability, the proposed method was applied to analyze rutin tablets and urine samples. One rutin tablet (20 mg/ tablet) was finely ground in a mortar and dissolved in anhydrous ethanol using an ultrasonic cleaner. The supernatant was diluted 100 times with 0.1 M PBS (pH 6.0) for use. In addition, a 1 mL urine sample was directly diluted 100 times with 0.1 M PBS (pH 6.0) without further pretreatment. The results are shown in Table 2. The recoveries were in the range of 95.2–101.4%. The results indicated that the GQDs@nano-CILE could be used to analyze actual samples.

Conclusions

In this paper, a rutin sensor based on GQDs@nano-CILE was constructed in a simple preparation process. A new electrode surface could be easily obtained by smoothing the electrode on the weighing paper. The graphene quantum dots/ionic liquid composites could increase the effective surface area and the conductivity of the sensor. Under optimal conditions, the modified electrode displayed high sensitivity to rutin. The wide linear range (5×10^{-9}–1×10^{-5} mol L^{-1}) and low detection limit (2×10^{-9} mol L^{-1}) were obtained. The method was successfully utilized to detect rutin in pharmaceutical preparations and biomedical fluids. It is of great significance for drug quality control and pharmacokinetic studies.

Table 2 Determination of rutin on GQDs@nano-CILE in real samples. ($n=3$[a])

Samples	Rutin tablets	Urine
Detected / μM	6.22	ND[b]
Added / μM	5.00	5.00
Found / μM	10.98	5.07
Recovery / %	95.2	101.4
RSD / %	1.81	4.46

[a]Three measurements were made for each sample
[b]Not detected

Author contribution Xinsheng Liu: visualization, writing—original draft preparation; Wenli Qiao: methodology, software, validation; Mengjun Chang: visualization, investigation; Yan Wang: software and editing, investigation; Yonghong Li: writing—reviewing, supervision.

Funding This research was supported by the Natural Science Foundation of Ningxia, China (No. 2022AAC03147).

Data availability This declaration is not applicable

Declarations

Ethical approval This declaration is not applicable.

Competing interests The authors declare no competing interests.

References

1. Ganeshpurkar A, Saluja AK (2017) The pharmacological potential of rutin. Saudi Pharm J 25:149–164
2. I.V. Koval'skii, I.I. Krasnyuk, I.I. Krasnyuk Jr., O.I. Nikulina, A.V. Belyatskaya, Yu. Ya. Kharitonov, N.B. Feldman, S.V. Lutsenko, (2014) Mechanisms of rutin pharmacological action (review). Pharm Chem J 48:73–76
3. Kicel A, Owczarek A, Michel P, Skalicka-Woźniak K, Kiss AK, Olszewska MA (2015) Application of HPCCC, UHPLC-PDA-ESIMS3 and HPLC-PDA methods for rapid, one-step preparative

separation and quantification of rutin in Forsythia flowers. Ind Crop Prod 76:86–94
4. Wu T, Yu C, Li R (2017) Determination of flavonoids in Flos Chrysanthemi and Flos Chrysanthemi Indici by capillary electrophoresis. Instrum Sci Technol 45:412–422
5. Wang Q, Ding F, Li H, He P, Fang Y (2003) Determination of hydrochlorothiazide and rutin in Chinese herb medicines and human urine by capillary zone electrophoresis with amperometric detection. J Pharm Biomed Anal 30:1507–1514
6. Xu H, Li Y, Tang HW, Liu CM, Wu QS (2010) Determination of rutin with UV-Vis spectrophotometric and laser-induced fluorimetric detections using a non-scanning spectrometer. Anal Lett 43:893–904
7. Gong A, Ping W, Wang J, Zhu X (2014) Cyclodextrin polymer/Fe_3O_4 nanocomposites as solid phase extraction material coupled with UV-vis spectrometry for the analysis of rutin, Spectrochim. Acta A 122:331–336
8. Nie Y, Tao X, Zhang H, Chai YQ, Yuan R (2014) Self-assembly of gold nanoclusters into a metal–organic framework with efficient electrochemiluminescence and their application for sensitive detection of rutin. Anal Chem 93:3445–3451
9. Kaleeswarran P, Koventhan C, Chen SM, Arumugam A (2022) Coherent design of indium doped copper bismuthate-encapsulated graphene nanocomposite for sensitive electrochemical detection of rutin. Colloid Surface A 643:128740
10. Elancheziyan M, Ganesan S, Theyagarajan K, Duraisamy M, Thenmozhi K, Weng C-H, Lin Y-T, Ponnusamy VK (2022) Novel biomass-derived porous-graphitic carbon coated iron oxide nanocomposite as an efficient electrocatalyst for the sensitive detection of rutin (vitamin P) in food and environmental samples. Environ Res 211:113012
11. Lu YL, Wang ZX, Mu XW, Liu YP, Shi Z, Zheng Y, Huang WS (2022) The electrochemical sensor based on Cu/Co binuclear MOFs and PVP cross-linked derivative materials for the sensitive detection of luteolin and rutin. Microchem J 175:107131
12. Li K, Liu W, Ni Y, Li D, Lin D, Su Z, Wei G (2017) Technical synthesis and biomedical applications of graphene quantum dots. J Mater Chem B 5:4811–4826
13. Disha P, Kumari MK, Nayak PK (2022) A bio-sensing platform based on graphene quantum dots for label free electrochemical detection of progesterone. Mater Today Proc 48:583–586
14. Arumugasamy SK, Govindaraju S, Yun K (2020) Electrochemical sensor for detecting dopamine using graphene quantum dots incorporated with multiwall carbon nanotubes. Appl Surf Sci 508:145294
15. Hatamluyi B, Es'haghi Z, Zahed FM, Darroudi M (2019) A novel electrochemical sensor based on GQDs-PANI/ZnO-NCs modified glassy carbon electrode for simultaneous determination of Irinotecan and 5-Fluorouracil in biological samples. Sensor Actuat B-Chem 286:540–549
16. Kunpatee K, Traipop S, Chailapakul O, Chuanuwatanakul S (2020) Simultaneous determination of ascorbic acid, dopamine, and uric acid using graphene quantum dots/ionic liquid modified screen-printed carbon electrode. Sensor Actuat B-Chem 314:128059
17. Li YT, Du C, Liu XS, Wang K, Yang HF, Li YH (2021) Non-enzymatic methyl parathion electrochemical sensor based on hydroxyl functionalized ionic liquid/zeolitic imidazolate framework composites modified glassy carbon electrode. J Electrochem Soc 168:077511
18. Li YH, Li YT, Jia LN, Li Y, Wang Y, Zhang PJ, Liu XS (2022) A simple sensor based on 1-butylpyridinium hexafluorophosphate@glassy carbon microspheres composites for the quantitative analysis of azo dyes. J Iran Chem Soc 19:1251–1260
19. Liu CQ, Huang JZ, Wang LS (2018) Electrochemical synthesis of a nanocomposite consisting of carboxy-modified multi-walled carbon nanotubes, polythionine and platinum nanoparticles for simultaneous voltametric determination of myricetin and rutin. Microchim Acta 185:414
20. Yang LT, Yang J, Xu BJ, Zhao FQ, Zeng BZ (2016) Facile preparation of molecularly imprinted polypyrrole-graphene multiwalled carbon nanotubes composite film modified electrode for rutin sensing. Talanta 161:413–418
21. Xing RM, Yang HT, Li SN, Yang JH, Zhao XY, Wang QL, Liu SH, Liu XH (2017) A sensitive and reliable rutin electrochemical sensor based on palladium phthalocyanine-MWCNTs-Nafion nanocomposite. J Solid State Electr 21:1219–1228
22. Arvand M, Shabani A, Ardaki MS (2017) A new electrochemical sensing platform based on binary composite of graphene oxide-chitosan for sensitive rutin determination, Food Anal. Method 10:2332–2345
23. Zou CE, Zhong JT, Li SM, Wang HW, Wang J, Yan B, Du YK (2017) Fabrication of reduced graphene oxide-bimetallic PdAu nanocomposites for the electrochemical determination of ascorbic acid, dopamine, uric acid and rutin. Electroanal Chem 805:110–119